

Adsorption and Thermal Decomposition of Acetaldehyde on Si(111)-7×7

Y. Bu, J. Breslin, and M. C. Lin*

Department of Chemistry, Emory University, Atlanta, Georgia 30322

Received: November 19, 1996[®]

The thermal stability of acetaldehyde on Si(111)7×7 was studied with HREELS, XPS, UPS, and TPD techniques. Acetaldehyde molecules were found to adsorb molecularly on the surface at 120 K, yielding HREELS peaks at 98, 124, 144, 185, and 380 and UPS peaks at 5.7, 7.6, 10.0, and 13.9 eV below E_f . Analysis of the XPS O_{1s} (shoulder at 531; 532 eV) and C_{1s} (288 and 285 eV) spectra indicated that the acetaldehyde was partially dissociated at 120 K. At ~350 K, the initial HREELS peaks at 185 and 144 meV diminished while peaks at 100 and 208 meV emerged, which indicated the desorption and/or dissociation of the C–C bond and the formation of Si–O and Si–CH₃ species. The UPS peaks at 5.7 and 10.0 eV diminished, and a new peak at 6.5 eV dominated the spectra from 350 to 1150 K. The parent mass was found by TPD to desorb at 320 K. At 500 K, the 100 meV HREELS peak vanished and a new peak at 270 meV became noticeable, indicating the breaking of the C–H bond and the formation of Si–H (D) species. TPD results indicated that H (D) species desorbed at around 800 K. By 1150 K, peaks at ~110 meV (HREELS) and ~7 eV (UPS) were the only significant features not found in the clean Si(111) spectra. In the XPS spectra, initial multiple features had converged by 350 K, and with increased temperature both the resulting O_{1s} and C_{1s} peaks shifted toward lower binding energy. By 1150 K, the O_{1s} peak had disappeared, leaving silicon carbide on the substrate.

Introduction

The adsorption and thermal decomposition of acetaldehyde on several metal surfaces have been studied under ultrahigh-vacuum conditions. These studies are useful for the elucidation of the Fischer–Tropsch reaction mechanism. Acetaldehyde was found to adsorb molecularly on Fe(100) with some dissociation at 185 K.¹ At elevated surface temperatures, CO, CH₃, and ethoxy intermediates, etc., were formed on the substrate. On Cu(110),^{2–4} CH₃CHO was found to adsorb molecularly on the clean surface at 80 K with evidence of structural transformation at 150 K. Oxidation products, such as CH₃COOH and acetate ions, were believed to be formed on an O-covered Cu(110) surface at 150 K. The reaction of acetaldehyde on Al-covered Cu(110) is even more complicated, and the processes depend on both surface temperature and Al coverage.² On Pt(100), Pt(110), and Pt(111),^{5,6} acetaldehyde was found to adsorb dissociatively on these surfaces, and C–C bond breaking and CO-like species were reported.

Catalytically-induced acetaldehyde reactions were also studied on CeO₂ surfaces,⁷ with and without partial Pd and/or Co metalization. On CeO₂ surfaces, acetaldehyde exhibited a variety of complex reaction mechanisms which include reduction to ethoxides, reductive coupling to form butene, oxidation to form acetates, and (β)-aldolization to form crotonaldehyde, while partial metalization of CeO₂ was found to enhance CO uptake of the substrate. Acetaldehyde has also been employed as a precursor in diamond thin-film deposition on Si(111), in which the H + CH₃CHO reaction was shown to be an efficient source of CH₃,⁸ a key reactive species in the diamond film deposition process.

Previously, we have investigated the surface chemistry of C-, N-, or O-containing small molecules, such as CH₃CO (CD₂-CO),⁹ CO,¹⁰ HCN (DCN),¹¹ NH₂CHO,¹² HN₃ (DN₃),¹³ and N₂H₄,¹⁴ on Si single-crystal surfaces. These studies helped us

to better understand the behavior of CH_x, NH_x, and OH_x species on Si substrates as well as the mechanisms for formation of Si carbide, Si nitride, and Si oxide. In order to facilitate the deposition of high-quality epitaxial layers on silicon, the characterization of the formation and thermal behavior of these compounds on Si substrates is a prerequisite to gaining a useful understanding of the growth process. The possible decomposition products of CH₃CHO on Si include molecules (e.g., CH₂-CO, CO, CH₃) which we have previously investigated. These results proved to be useful reference points for interpreting the data reported in this article, in which we present the high-resolution electron energy loss spectroscopy (HREELS), X-ray photoelectron spectroscopy (XPS), temperature-programmed desorption (TPD) and ultraviolet photoelectron spectroscopy (UPS) results for acetaldehyde on Si(111)7×7.

Experimental Section

The experiment was carried out in an ultrahigh-vacuum (UHV) system (Leybold, Inc.) with a base pressure of 5×10^{-11} Torr. The system is equipped with HREELS, XPS, UPS, Auger electron spectrometer (AES), TPD, and low-energy electron diffractometer (LEED) as described elsewhere.^{9–14} In the HREELS measurement, a 5 eV electron beam was used, and its full width at half-maximum (fwhm) was 7 meV in the straight-through mode. However, after scattering from a clean Si(111)7×7 surface at 120 K, the fwhm of the beam broadened to 12 meV. An Al X-ray source was used for the XPS spectra, and the pass energy was set at 50 eV to give a resolution of <1.4 eV. A helium discharge lamp provided the 21.1 (He I) and 40.8 eV (He II) photon beams for the UPS study. The TPD experiment was carried out with a residual gas analyzer (VG Sensorlab 220). A reverse-view LEED instrument was used to characterize the clean surface structure.

Si(111) single-crystal wafers from Virginia Semiconductor Corp. were cut into 1.5×1.0 cm samples which were cleaned with a hot 5% HF solution and rinsed with deionized water. The samples were then transferred into the UHV chamber and

* Corresponding author. e-mail address: chemmcl@emory.edu.

[®] Abstract published in *Advance ACS Abstracts*, February 1, 1997.

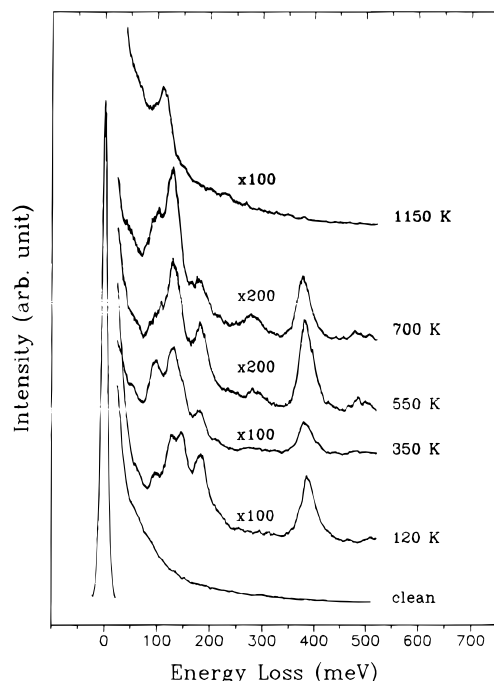


Figure 1. HREELS of CH_3CHO on $\text{Si}(111)-7\times 7$. The surface was exposed to CH_3CHO at 120 K and then heated at the indicated temperatures. All spectra were recorded at 120 K.

heated at $T_s \cong 1500$ K repeatedly until no C, O, N, or other impurities could be detected by XPS, AES, and HREELS. The samples prepared in this manner also showed sharp 7×7 LEED patterns.

The high-purity acetaldehyde- h_4 , $-d_1$, and $-d_4$ samples from Aldrich were purified by vacuum distillation. FTIR spectroscopy was used to check D enrichment for CH_3CDO and CD_3CDO samples. On the basis of the FTIR measurement, we found that the D enrichment is $>95\%$ in CH_3CDO and CD_3CDO . The acetaldehyde was introduced into the UHV chamber through 1/8 in. o.d. stainless steel tubing which had a flared tip with an i.d. of $\sim 1/4$ in. to achieve even coverage when the surface was moved close for TPD dosing. After the dosing line was repeatedly purged with acetaldehyde, the surface was moved in front of the doser. The dosages were estimated according to the pressure reading from an ion gauge.

Results

Figure 1 shows HREELS spectra of CH_3CHO on $\text{Si}(111)-7\times 7$. After the surface was exposed to 1 langmuir (L) of CH_3CHO at 120 K, HREELS showed peaks at 98, 124, 144, 185, and 380 meV. By analogy to IR/Raman results for gaseous/liquid CH_3CHO ,^{16–20} listed in Table 1, we assigned these peaks to CH bending, CH_3 rocking, C–C stretching and CH_3 symmetric deformation, and CH stretching vibrations, respectively. In addition, a rather weak hump at ~ 58 meV was noted. This hump could be attributed to the CCO deformation vibrational mode. The CO stretching mode, expected at 217 meV, was not well-resolved in the spectrum. However, it was observed in the corresponding CD_3CDO HREELS spectrum, where the adjacent, more intense CD_3 and CD vibrational modes shifted toward lower frequencies.

When the sample was heated to 250 K, there were no obvious changes in the CH_3CHO HREELS spectrum. In contrast, the following changes were noted at 350 K: (1) The 144 meV peak due to the C–C stretching and CH_3 symmetric deformation modes virtually disappeared; (2) the 185 meV peak became weaker; (3) an intense peak appeared at ~ 100 meV, and the

TABLE 1: Vibrational Frequencies (in meV) of Gaseous/Liquid Acetaldehyde and Acetaldehyde on $\text{Si}(111)-7\times 7^a$

mode	no.	$\text{CH}_3(\text{D}_3)\text{CH}(\text{D})\text{O}$		$\text{CH}_3(\text{D}_3)\text{CH}(\text{D})\text{O}^d$ on $\text{Si}(111)$ at 120 K
		gaseous ^b	liquid ^c	
CH_3 stret	ν_1	373 (281)	373	
	ν_2		362 (264)	380 (263)
CH stret	ν_3	350 (256)	373 (257)	
CO stret	ν_4	216	213 (212)	212 (~ 200)
CH_3 deform	ν_5	179 (130)	177 (135)	185 (140)
	ν_{12}	168 (128)	167 (127)	
CH bend	ν_6	174 (138)	173 (138)	
	ν_{14}	95 (83)	95 (83)	98 (88)
CC stret	ν_8	138 (129,143)	138 (134)	144 (~ 135)
CH_3 rock	ν_9	114 (93)	113 (93)	124 (~ 90)
CCO deform	ν_{10}	65 (54)	64 (52)	58

^a 1 meV = 8.066 cm^{-1} . ^b References 16, 17, 19, and 20. ^c References 16–19. ^d This work.

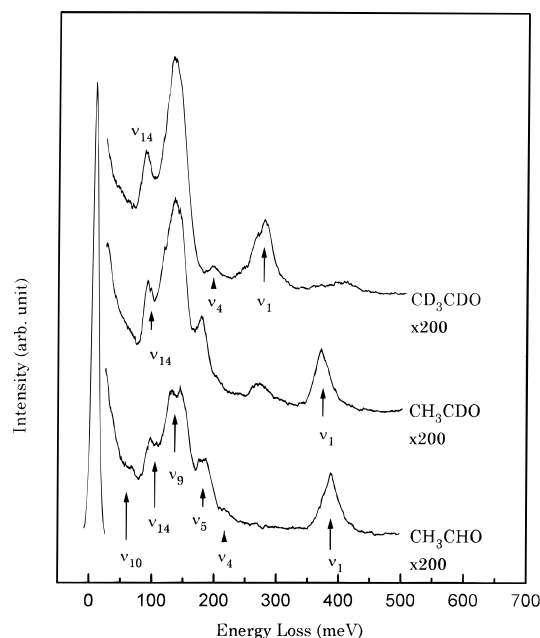


Figure 2. HREELS of CH_3CHO (bottom), CH_3CDO , and CD_3CDO (top) on $\text{Si}(111)-7\times 7$ at 120 K. The spectra were prepared and recorded under the same conditions as those in Figure 1. Vibrational assignments are given in Table 1 and discussed in the text.

CO stretching mode at 208 meV became noticeable. At 550 K, the 100 meV peak vanished, and a weak mode at 270 meV due to the Si–H stretching vibration appeared in the spectrum. Further heating the sample at 700 K caused no significant changes except the decrease in the intensity of the CH_x -related modes and the concomitant increase in the Si–H mode. Finally, at 1150 K, the HREELS spectrum was dominated by a peak at ~ 110 meV, indicating the formation of silicon carbide.^{9,15}

The 120 K HREELS spectra taken from CH_3CHO , CH_3CDO and CD_3CDO on $\text{Si}(111)-7\times 7$ are shown in Figure 2. The expected peak shifts upon deuteration were observed, and the assignments of the vibrational modes are listed in Table 1 together with the IR/Raman results for gaseous/liquid acetaldehyde.^{13–20} In comparison with the 120 K CH_3CHO HREELS spectrum, the two CH bending modes for CH_3CDO shifted from 98 and 185 meV to 88 and ~ 140 meV, respectively. The latter peak overlapped with the CC stretching and CH_3 symmetric deformation modes to give a broad peak centered at ~ 138 meV. Meanwhile, the relative intensity of the 185 meV peak became weaker, and a corresponding CD stretching vibrational peak appeared at 263 meV. In the CD_3CDO spectrum, the rocking, asymmetric deformation, and stretching peaks of the methyl group shifted from 124, 185, and 370 meV

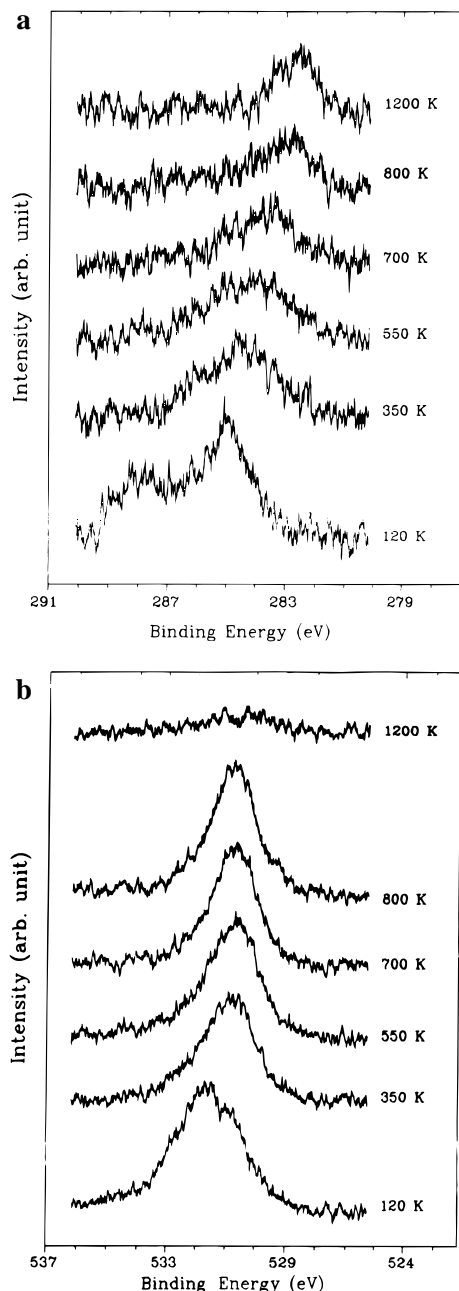


Figure 3. XPS spectra of C_{1s} (a) and O_{1s} (b), using an Al X-ray source. The Si(111) surface was dosed and heated under the same experimental conditions as those in Figure 1.

to 88, 130, and 280 meV, respectively. Accompanying these changes, the CO stretching mode became better resolved because of the red shift of the CH₃ deformation mode at 185 meV. The CD₃ deformation mode expected at 130 meV overlapped with the CD bending and CC stretching vibrational modes.

The thermal effect on the CH₃CDO and CD₃CDO HREELS spectra was less clear, because the CC stretching mode overlapped with some of the CD-related vibrations. Heating the sample at 250 K caused no obvious change in either CH₃CDO or CD₃CDO spectra. At 350 K, a slight decrease in the ~130 meV peak intensity was noted. Above 500 K, the lower frequency part (<130 meV) of the HREELS spectra was similar for CH₃CHO, CH₃CDO, and CD₃CDO, suggesting that these vibrations are attributable to SiO and SiC species.

Shown in Figure 3 are the C_{1s} (a) and O_{1s} (b) XPS spectra. When the Si(111)7×7 surface was exposed to 1 langmuir of CH₃CDO at 120 K, O_{1s} XPS showed a broad peak at 531.7 eV with some contribution from a lower binding energy component,

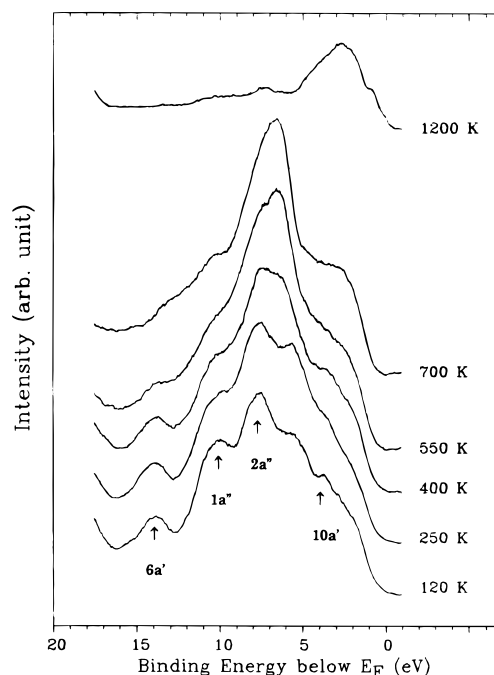


Figure 4. UPS results of CH₃CHO on Si(111)-7×7. He II (40.8 eV) photon beam was used for the spectra recording, with molecular CH₃CHO peak assignments^{2,3} indicated. All the other experimental conditions were the same as those in Figure 1.

while C_{1s} XPS showed two peaks at 287.8 and 285.0 eV, respectively. After the sample was heated to 250 K, no obvious changes were observed in the C_{1s} and O_{1s} XPS spectra. However, at 350 K the two C_{1s} peaks merged to give one broad band centered at ~284.5 eV, the O_{1s} peak shifted to 530.8 eV, and the overall intensity decreased for C_{1s} and O_{1s} XPS peaks. Heating this sample at higher temperatures caused a continuous shift of the C_{1s} peak toward lower binding energy. At 700 K, the C_{1s} and O_{1s} XPS peaks located at 283.5 and 530.7 eV, respectively. Finally, at 1150 K the C_{1s} XPS peak shifted to 282.7 eV due to the formation of SiC, while the O_{1s} XPS peak practically vanished because of the desorption of the O-containing species.

The thermal effect on He II UPS spectra of CH₃CHO/Si-(111) was also studied, and the results are displayed in Figure 4. When a Si(111) surface was exposed to ~1 langmuir of CH₃CHO at 120 K, peaks at 5.7, 7.6, 10.0, and 13.9 eV below E_F (Fermi level) appeared in the UPS spectrum. By analogy to the UPS results of the gaseous CH₃CHO and CH₃CHO on Cu(110), we attributed these peaks to 10a', 2a'', 1a'', and 6a' molecular orbitals, respectively.^{2,3} No changes were observed at 250 K. However, at 400 K peaks at 5.7 and 10.0 eV became weaker, and a broad band around 6.5 eV dominated the UPS spectrum. This feature continued to dominate the spectrum up to 700 K. At 1150 K, the 6.5 eV peak vanished, and the spectrum was similar to that taken from a clean surface, except for a small hump at ~7 eV, which is attributable to the SiC species.^{15,22}

Figure 5a shows the TPD results of CD₃CDO on Si(111)7×7 at the indicated dosages. In order to reduce the spectral interference from molecules absorbed on the sample holder (which showed a lower temperature peak at ~200 K), the surface was moved to within ~2 mm of the inlet nozzle while dosing. Thus, it was not possible to estimate the sample exposure by the ion gauge reading. On the basis of our XPS data (Si XPS signal attenuation), we estimated that the acetaldehyde coverage is ~0.4 at an exposure of 45 s. When we incrementally increased the dosage, the magnitude of the TPD signal increased at a rate somewhat higher than a linear dosage

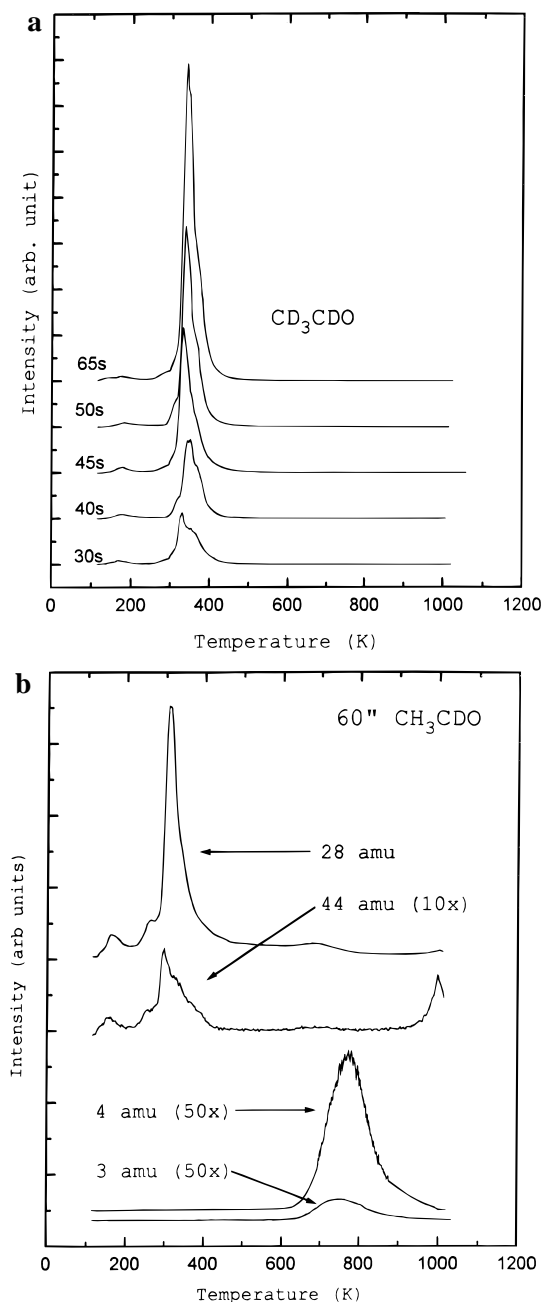


Figure 5. (a) TPD for $m/e = 48$ (CD_3CDO) at the indicated dosing time. The relative coverage is discussed in the text. (b) TPD of CH_3CDO on $\text{Si}(111)7\times7$ for $m/e = 3, 4, 28$, and 44 . The $\text{Si}(111)$ surface was exposed to CH_3CDO at 120 K for 60 s.

dependence would predict. We speculate that this is due to an initial consumption of parent molecules by the dosing line as they first enter the vacuum chamber. The parent mass ($m/e = 48$) showed a single peak at ~ 320 K. At lower coverages, there is a shoulder at ~ 350 K.

At higher temperatures, other fragments were observed as shown in Figure 5b. For CH_3CDO , $m/e = 3$ (DH) and $m/e = 4$ (D_2) showed single peaks at 750 K due to the desorption of the surface hydrogen. In the corresponding CD_3CDO experiment, $m/e = 4$ also showed a single peak at 750 K with a much smaller peak at ~ 300 K, presumably caused by the cracking of the parent molecules in the RGA. For $m/e = 44$, two major components at ~ 320 and ~ 1000 K were evident in the spectrum.

Discussion

The thermal stability of acetaldehyde adsorbed on $\text{Si}(111)7\times7$ was studied by using HREELS, XPS, UPS, and TPD techniques.

The molecular adsorption of acetaldehyde on the $\text{Si}(111)$ surface at 120 K was clearly evident in HREELS and UPS. In the CH_3CHO HREEL spectrum, all the molecular vibrations were observed and compared with the IR/Raman results for the gaseous/liquid CH_3CHO (see Table 1). Some of the modes were not resolved in the spectrum with the resolution used in this study. However, with the aid of the spectra taken from CH_3CDO and CD_3CDO , the assignment of each mode is fairly straightforward. For example, the 185 meV peak for CH_3CHO is composed of CH_3 deformation and CH bending modes. In the CH_3CDO spectrum, the relative intensity of the 185 meV peak decreased and the 140 meV peak became broader because the CH bending mode shifted from 185 to ~ 140 meV. In the corresponding CD_3CDO spectrum, the 185 meV peak vanished due to the shift of CH deformation mode from ~ 180 to 130 meV.

In the C_{1s} XPS spectrum, the C_{1s} signal showed two peaks at 285.0 and 287.8 eV. They are from the carbon atoms in CH_3 and C(H)=O groups, respectively. Similarly, two C_{1s} XPS peaks were observed for the acetaldehyde on $\text{Fe}(100)$ and $\text{Cu}(110)$ surfaces. In the case of $\text{CH}_3\text{CHO}/\text{Fe}(100)$,¹ the lower BE peak was more intense than the higher BE one, and the peak intensity difference was attributed to the partial dissociation of the molecules upon adsorption. In the present study of CH_3CHO on $\text{Si}(111)7\times7$, we also noticed that the two C_{1s} XPS peak intensities were different. This may indicate a partial dissociative adsorption of acetaldehyde on $\text{Si}(111)$. The argument is consistent with the high-temperature XPS result, e.g., at 350 K, where the C_{1s} XPS shows a single broad peak at 284.5 eV due to the breaking of the C–C bond (see later discussion). Furthermore, the O_{1s} XPS peak shows some contribution from the 530.8 eV component, which becomes the dominant feature at temperatures above 350 K. On the other hand, the difference in C_{1s} XPS peak intensity at <250 K may be partially due to the adsorption geometry; i.e., the carbonyl C atom is bonded to the surface with the methyl group with the O atom pointing toward vacuum. Thus, a scattering attenuation effect was expected for the carbonyl carbon atom.

As to the surface binding sites, we noticed that upon being exposed to CH_3CHO molecules, the S_2 surface states attenuated first and then the S_1 states. These changes were shown in the He I UP spectra (see Figure 6). The S_1 and S_2 surface states originate from the Si dangling bonds on adatoms and rest atoms, respectively, with the Si adatoms being the topmost layer. In the studies of NH_3 on $\text{Si}(111)7\times7$, Avouris et al.²¹ found that the signals from the rest atoms attenuated first and then the adatoms when the surface was exposed to an increasing amount of NH_3 molecules. On the other hand, for $(\text{CH}_3)_3\text{In}$ (TMIn)²² and ketene on $\text{Si}(111)7\times7$,⁹ we found that the S_1 surface states diminished before the S_2 surface states did when the surface was exposed to more TMIn or ketene. These observations suggest that S_1 and S_2 surface states have different chemical binding affinity toward various molecules. In our TPD measurements, a desorption peak at 320 K with a shoulder at 350 K was observed for the parent mass ($m/e = 48$) at lower dosages. We speculate that these two components may be related to the S_1 and S_2 states. Further experiments are needed to confirm this speculation.

When the sample was heated at ~ 250 K, no obvious changes were observed in HREELS, UPS, or XPS. At 350 K, a slight decrease of C_{1s} and O_{1s} XPS peak intensities indicates a partial desorption of the adspecies. Indeed, a desorption peak for the parent molecule was observed at ~ 320 K in our TPD measurements. Meanwhile, the two C_{1s} XPS peaks merged to give a single peak centered at 284.5 eV and O_{1s} XPS peaks shifted

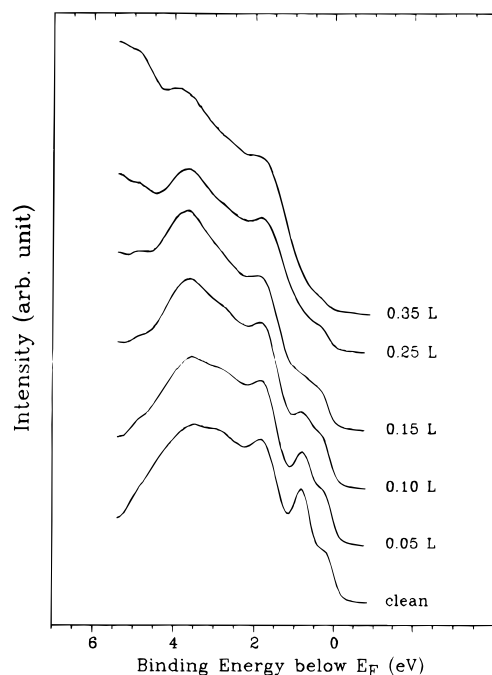
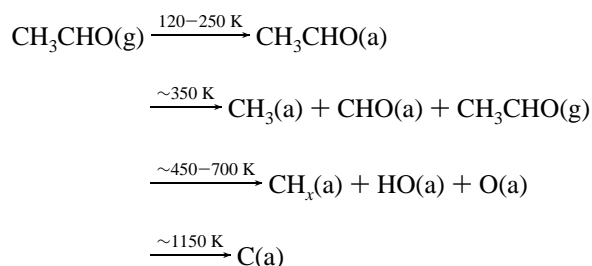


Figure 6. He I (21.2 eV) UPS results of CH_3CHO on $\text{Si}(111)\text{-}7\times 7$. The surface was dosed at 120 K as indicated. The S_1 and S_2 surface states decreased as the surface was exposed to increasing amounts of CH_3CHO molecules.

from 531.7 to 530.8 eV. In HREELS, the C–C stretching mode at 144 meV virtually disappeared, while an intense peak at ~ 100 meV appeared in the spectrum. A peak at 105 meV was observed in our earlier study of TMIn on $\text{Si}(111)7\times 7$ when the surface was heated to 520 K to break the In–C bonds.²² The peak was assigned to the CH_3 deformation mode for the CH_3 group on $\text{Si}(111)7\times 7$, which was discussed in detail in ref 22. Another intense peak at 128 meV is likely due to the Si–O bond, which persisted up to 700 K, while a small hump appeared at ~ 208 meV, which is red-shifted by more than 10 meV as compared to a normal carbonyl CO double bond. This red shift, coupled with the 128 meV Si–O stretching mode and the observed C_{1s} XPS peak shifting, indicates the formation of the Si–O bond and thus the weakening of the CO bond. In the corresponding UPS spectra, the two peaks at 5.7 and 10.0 eV due to $10a'$ and $1a''$ molecular orbitals attenuated significantly, and a new peak at ~ 6.5 eV was noted. The 5.7 eV peak is associated with the O lone electron pairs; its peak intensity decrease suggests the formation of an Si–O bond, which is consistent with the HREELS results discussed above. The 10.0 eV peak has the character of a π CH_3 bond, and its peak intensity attenuation is likely due to the C–C bond breaking and the migration of the CH_3 group from CH_3CHO onto the substrate. The appearance of the new 6.5 eV peak is attributable to the formation of the Si–C bond (i.e., Si– CH_3 species) and the Si–O bond. The aforementioned changes in both HREELS and UPS indicate the break of the C–C bond and the formation of Si– CH_3 species at 350 K.

Further heating the sample to 550 K caused the disappearance of the ~ 100 meV HREELS peak and the appearance of a new peak at ~ 270 meV attributable to the Si–H stretching mode. These simultaneous changes indicate the cracking of the CH bond and the formation of the Si–H species. The Si–H stretching mode at ~ 270 meV, being a little higher than that of ~ 260 meV for H on a clean Si surface, is probably caused by the Si atoms back-bonded to O atoms. At higher temperatures, CH_x -related features decreased in intensity, indicating a further breaking of the CH bond. Above 800 K, the HREELS spectra

for all acetaldehyde isotopes are dominated by a single peak at 110 meV, which can be ascribed to the formation of SiC,²² while the Si–O stretching mode at 128 meV vanished. In the corresponding XPS results, the O_{1s} XPS peak virtually disappeared, and the C_{1s} XPS peak shifted to 282.8 eV at >800 K. In the UPS spectra, the intense peak at ~ 6.5 eV diminished and the spectrum at 1150 K was similar to that of the clean surface, except for the presence of a weak Si–C feature at ~ 7 eV. In the TPD measurement, two peaks were noted for the $m/e = 44$ at ~ 320 and ~ 1000 K. The lower temperature one (~ 320 K) follows the parent profile, while the higher temperature one (~ 1000 K) is attributed to the SiO species. This observation is consistent with our surface analysis results, where the O-related features, e.g., O_{1s} XPS peak and the 128 meV peak in HREELS, practically vanished above 1000 K. We also examined the possible product CO ($m/e = 28$), but the results were not conclusive. As can be seen in Figure 5b, the dominant peak at ~ 320 K again follows the parent profile, while a small hump at ~ 680 K was not observed in the parent spectrum. However, a similar hump was evident in the $m/e = 44$ (SiO) spectrum; this hump may have resulted from Si^+ ion fragment. The decomposition process described above can be summarized as follows:



Conclusion

The adsorption and thermal decomposition of CH_3CHO , $\text{CH}_3\text{-CDO}$, and CD_3CDO on $\text{Si}(111)7\times 7$ have been studied with HREELS, XPS, TPD, and UPS. Acetaldehyde was found to adsorb molecularly on the surface at 120 K. However, some dissociative adsorption may also have occurred according to our XPS results. No obvious changes were noted when the sample was heated to 250 K. At 350 K, on the other hand, the breaking of the C–C bond, the formation of the Si–O bond, and the CH_3 groups on the surface were indicated by HREELS and UPS spectra. A partial desorption of the parent molecule was also revealed by the decrease of the C and O XPS peak intensity and the appearance of a desorption peak at ~ 320 K for the parent molecule. Further heating the sample to 700 K caused the decomposition of the CH_3 adspecies and the formation of Si–H species. Finally, at 1150 K, O-containing species and H adspecies desorbed from the surface, while C remained on the substrate to form silicon carbide.

Acknowledgment. The authors gratefully acknowledge the support of this work by the Office of Naval Research.

References and Notes

- (1) Benziger, J. B.; Madix, R. J. *J. Catal.* **1982**, *74*, 55.
- (2) Prabhakaran, K.; Rao, C. N. R. *Appl. Surf. Sci.* **1990**, *44*, 205.
- (3) Yashonath, S.; Basu, P. K.; Srinivasan, A.; Hegde, M. S.; Rao, C. N. R. *Proc.-Indian Acad. Sci., Chem. Sci.* **1982**, *91*, 101.
- (4) Bowker, M.; Madix, R. J. *Vacuum* **1981**, *31*, 711.
- (5) Cases, F.; Vazquez, J. L.; Perez, J. M.; Aldaz, A.; Clavilier, J. *J. Electroanal. Chem. Interfacial Electrochem.* **1990**, *281*, 283.
- (6) Perez, J. M.; Cases, F.; Vazquez, J. L.; Aldaz, A. *New J. Chem.* **1990**, *14*, 679.
- (7) Idriss, H.; Diagne, C.; Hiderman, J. P.; Kiennemann, A.; Barteau, M. A. *J. Catal.* **1995**, *155*, 219.

- (8) Apkarian, P. P.; Tarr, J. T.; Kaufman, M. J.; Menger, F. M. *Proc. Microsc. Microanal.* **1995**, 860.
- (9) Bu, Y.; Lin, M. C. *J. Chin. Chem. Soc. (Taipei)* **1995**, 42, 309.
- (10) Bu, Y.; Lin, M. C. *Surf. Sci.* **1993**, 298, 94.
- (11) (a) Bu, Y.; Ma, L.; Lin, M. C. *J. Phys. Chem.* **1993**, 97, 7081. (b) Bu, Y.; Ma, L.; Lin, M. C. *J. Phys. Chem.* **1993**, 97, 11797.
- (12) Bu, Y.; Lin, M. C. *Langmuir* **1994**, 10, 3621.
- (13) (a) Bu, Y.; Chu, J. C. S.; Lin, M. C. *Surf. Sci. Lett.* **1992**, 264, L151. (b) Bu, Y.; Lin, M. C. *Surf. Sci.* **1994**, 301, 118.
- (14) Bu, Y.; Shinn, D. W.; Lin, M. C. *Surf. Sci.* **1992**, 276, 184.
- (15) Froitzheim, H.; Köhler, U.; Lammering, H. *Phys. Rev.* **1984**, B30, 5771.
- (16) Morris, J. C. *J. Chem. Phys.* **1943**, 11, 230.
- (17) Cossee, P.; Schachtschneider, J. H. *J. Chem. Phys.* **1966**, 44, 97.
- (18) Wood, R. W. *J. Chem. Phys.* **1936**, 4, 536.
- (19) Evans, J. C.; Bernstein, H. J. *Can. J. Chem.* **1956**, 34, 1084.
- (20) Fateley, W. G.; Miller, F. A. *Spectrochim. Acta* **1963**, 19, 389.
- (21) Avouris, Ph.; Wolkow, R. *Phys. Rev.* **1989**, B39, 5091.
- (22) Bu, Y.; Chu, J. C. S.; Lin, M. C. *Mater. Lett.* **1992**, 14, 207.